

PEDOT:PSS thin film for photovoltaic application

J. Weszka ^{a,b}, M.M. Szindler ^{a,*}, P. Jarka ^a

^a Institute of Engineering Materials and Biomaterials,

Silesian University of Technology, ul. Konarskiego 18a, 44-100 Gliwice, Poland

^b Department of Physics, Centre of Polymer and Carbon Materials,

Polish Academy of Sciences, ul. M. Curie-Skłodowskiej 34, 41-819 Zabrze, Poland

* Corresponding e-mail address: magdalena.szindler@polsl.pl

Received 22.05.2013; published in revised form 01.08.2013

Materials

ABSTRACT

Purpose: The aim of this paper was to investigate changes in surface morphology and optical parameters of thin films of poly(3,4-ethylenedioxythiophene) poly(styrenesulfonate) (PEDOT:PSS). Thin films were prepared using spin coating method.

Design/methodology/approach: The thin films of PEDOT:PSS was investigate by Raman scattering technique in Raman spectrometer. The changes in surface topography were observed with the atomic force microscope AFM XE-100. The results of roughness have been prepared in the software XEI Park Systems. The measurement of optical parameter was performed using spectrometer UV/VIS and spectroscopic ellipsometer.

Findings: Results and their analysis allow to conclude that the PEDOT:PSS solution concentration and spin speed, an important factor in spin coating technology, have a significant influence on surface morphology and optical reflection of thin films.

Practical implications: Knowledge about the sol gel PEDOT:PSS optical parameters and the possibility of obtaining a uniform thin films show that it can be good material for photovoltaic and optoelectronic devices.

Originality/value: The paper presents some researches of PEDOT:PSS thin films deposited by spin coating method on glass substrate

Keywords: Electroconductive polymer; Polyelectrolyte; PEDOT:PSS; Organic solar cells; spin coating

Reference to this paper should be given in the following way:

J. Weszka, M.M. Szindler, P. Jarka, PEDOT:PSS thin film for photovoltaic application, Journal of Achievements in Materials and Manufacturing Engineering 59/2 (2013) 59-66.

1. Introduction

Most polymers which are widely used in industry and the everyday life belong to the typical insulators. However, electrically conductive polymers are exist too. They are already known since the mid-nineteenth century, but their practical importance, until recently, been underestimated [1-7].

In works from the 60s of the last century showed greater possibilities of their practical application. Thanks to their properties, they can be used in electronics, sensors, electrochemical cells, and many others, which draws attention

engineers and electrochemists. In 2000 A.G. MacDiarmid, A.J. Heeger and H. Shirakawa they received the Nobel Prize in Chemistry for work on polyacetylene [5-11].

There are three basic types of conductive polymers, with different conduction mechanism [1,9-11]:

- ionically conductive polymers, where polymer chain has no conductive itself properties, and the conductive factor is an electrolyte (e.g., lithium chlorate);
- conductive polymers based on the mechanisms of oxidation and reduction (redox) conductivity of these polymers is hopping of electrons between redox centers of the polymer;

- electronically conductive polymers, in this case, the electron transport system is in the conjugated double bonds of the polymer chain.

Spite of the short development in this area, now are known tens of electroconductive polymers (including derivatives thereof). The most important are polyacetylene, polyaniline, polypyrrole and polythiophene [1,3-7].

The first of these - polyacetylene, can exist in two isomeric forms, cis or trans (Fig. 1). Cis form is thermodynamically unstable and at elevated temperature is spontaneously transformed into a trans. Conductivity of pure polyacetylene is as small as 10^{-9} S/cm in the case of the cis form and lead to 10^{-4} S/cm where the second prevails in a sample of possible configurations. After doping conductivity increases by up to 13 orders of magnitude. Polyacetylene can be prepared by electrochemical, therefore developed several methods for chemical synthesis, is a major synthesis using Ziegler-Natta catalysts. Depending on the quantity of catalyst used, we can get the black powder or silver film, which after doping it turns color to gold. Unfortunately doped polyacetylene is unstable in atmospheric conditions, so its use is limited to closed systems as batteries [1,3-7,9-13].

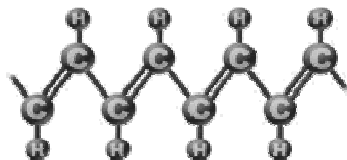


Fig. 1. Structural formula of the trans form polyacetylene [1,10]

Low stability of electro conductive polymers is really the biggest disadvantage. One of the most time-stable polymer is polyaniline, called aniline black, which is known since the nineteenth century and it is one of the most researched electro conductive polymers. The chain of polyaniline (Fig. 2) is composed of oxidized and reduced segments, which is important because only the most oxidized form shows an electrical conductivity after doping. Usually polyaniline is obtained by oxidation of the aniline on the anode in an acid medium, its conductivity after doping reaches 10^4 S/cm. Polyaniline requires the transformation of the processable form of what is being done by protonation of the appropriate acids. It is used, among others as protective coatings, anti-static material, the components of coatings, which can adsorb radar waves, PLED displays, heterogeneous catalysts [1,3-7,14-17].

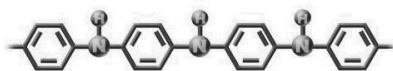


Fig. 2. Polyaniline structural formula [1,7]

Polypyrrole (Fig. 3) is another very important conductive polymer due to its properties. It shows a significant current stability, and most importantly, it is stable at atmospheric conditions and the water environment, and it is characterized by a very high biocompatibility. It is produced mainly by means of the application of electrochemically platinum or ITO electrode. It is used in batteries, accumulators, as the conductive composites

(mainly heating elements), biosensors, as well as a metal corrosion inhibitor [3-7,9,16].

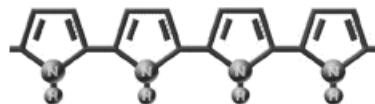


Fig. 3. Polypyrrole structural formula [1,7]

The fourth conductive polymer belongs to the group of the most important is polythiophene and its derivatives. These have very good chemical resistance. It is possible to modify the properties of the polymer wide by interference with the structure of the monomer. By this method it is possible to obtain derivative of polythiophene, 3,4-ethylenedioxythiophene, which is called. PEDOT [1,3-8,14,15-19].

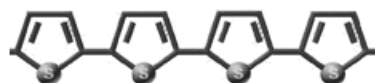


Fig. 4. Polythiophene structural formula [1,8]

PEDOT:PSS is a polymer blend that consists of a conducting poly(3,4-ethylenedioxythiophene) and poly(styrenesulfonate). PEDOT is a polycation and PSS is a polyanion [15-19].

2. Materials and methodology

The PEDOT:PSS thin films were prepared by the sol-gel spin coating technique. Deionized water was used as a solvent. The solutions were prepared with different ratio between PEDOT:PSS and deionized water (Table 1).

Table 1.

The adopted symbols of solutions and thin films PEDOT:PSS			
Solution	Concentration of the solution PEDOT:PSS/water	Sample	Spin speed [rpm]
P	100/0	P2	2000
		P4	4000
R	70/30	R2	2000
		R4	4000
S	50/50	S2	2000
		S4	4000
T	30/70	T2	2000
		T4	4000

The Raman spectra were obtained from sol-gel solutions by Raman scattering technique. The Raman spectra were taken on Renishaw inVia Reflex Raman microscope with $\lambda=514$ nm line of 10 mW power output. The data were collected with a 10 s data point acquisition time in the spectral region of $100-3200$ cm^{-1} .

Thin films were prepared from four different solution by spin coating method. The solutions were spin coated with two spin speed (2000 and 4000 rpm) on the glass substrates. Thin films were obtained on POLOS Spin 150 spin coater.

The changes in surface topography were observed with the atomic force microscope AFM XE-100 in none-contact mode. Under the microscope, we observed an area of 1x1 μm . The results of roughness have been prepared in the software XEI Park Systems.

UV/VIS spectra were recorded within 300-800 wavelength interval with JASCO 570 spectrometer.

Thickness and refractive index were determined with SENTECH ellipsometer. The used spectral range was 250-850 nm. The samples were measured at a fixed angle of incidence of $\Phi=70^\circ$.

3. Results and discussion

The Raman spectra (Figs. 5-8) show bands in Raman shift typical for PEDOT:PSS. The relative intensities of them depends on the resonance Raman effect, the amount of each polymer and water.

Fig. 5 show Raman spectra of the PEDOT:PSS prepared from solution P. We can see peaks from PEDOT and from PSS. Here the peaks are the most pronounced than the peaks obtained from solution T, shown on Fig. 8. This is due to the changes in the concentration of PEDOT:PSS in each of this solution.

The study of the surface topography was performed by atomic force microscope AFM XE-100 working in a non-contact mode. All images were taken on the 1x1 μm^2 area. Figs. 9-16 shows three - dimensional surface topography of PEDOT:PSS thin films. Three-dimensional AFM images were also presented as a graphic 3D images (Figs. 17-24). The thin films were deposited with two

spin speed and with the solutions of different concentrations with water. Fig. 9 show image topography of thin film obtained from solution P with spin rate 2000 rpm. We can observe marginal irregularities occurring on the surface of the layer. These irregularities are in the range of a few nm (Fig. 25). Fig. 10 show image topography of thin film obtained from the same solution P but with spin rate 4000 rpm. Here we have biggest irregularities than previous picture (Fig. 26). We saw that with the increase in the spin rate in this case there are larger differences in the surface topography PEDOT:PSS thin film. The more clear you can see it in the 3D pictures (Fig. 17 and Fig. 18).

The roughness results was made in the XEI software (Figs. 25-32). The best results were obtained for samples P2 and R2 (Figs. 25, 27) characterized uniform surface topography without any precipitates. The worst result was obtained for the sample P4 (Fig. 26) characterized by the presence of large precipitates on the surface exceeding 26 nm (Table 2).

Table 2.

The roughness parameters of a PEDOT:PSS thin films

Sample	Max Height [nm]	R _q [nm]	R _a [nm]
P2	3.805	0.981	0.783
P4	26.158	4.159	2.091
R2	6.048	0.882	0.676
R4	19.179	2.023	1.122
S2	12.904	1.391	0.742
S4	8.664	1.057	0.723
T2	6.351	1.266	0.986
T4	9.597	1.371	1.014

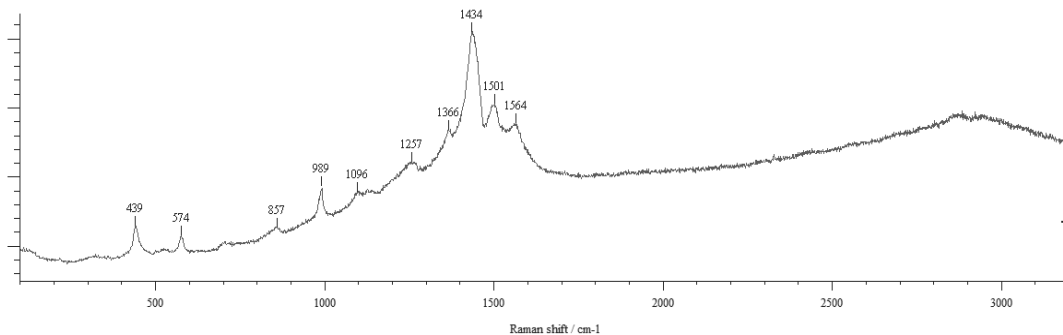


Fig. 5. Raman spectra of the PEDOT:PSS prepared from solution P

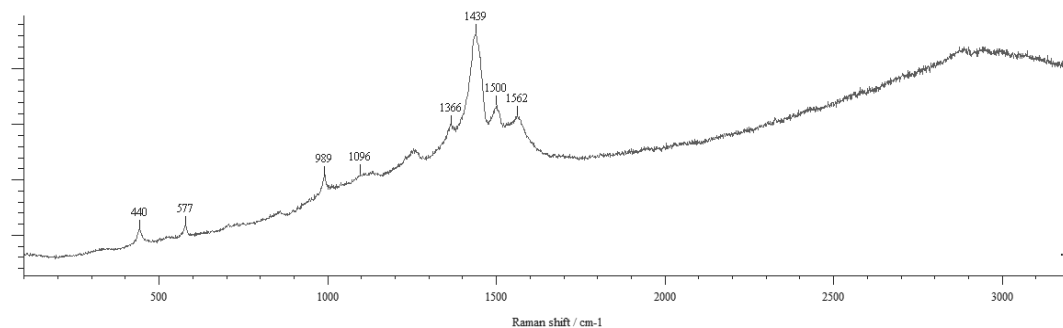


Fig. 6. Raman spectra of the PEDOT:PSS prepared from solution R

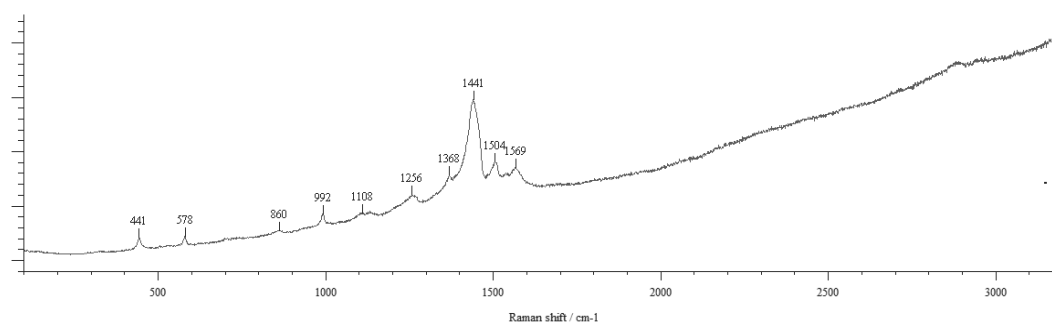


Fig. 7. Raman spectra of the PEDOT:PSS prepared from solution S

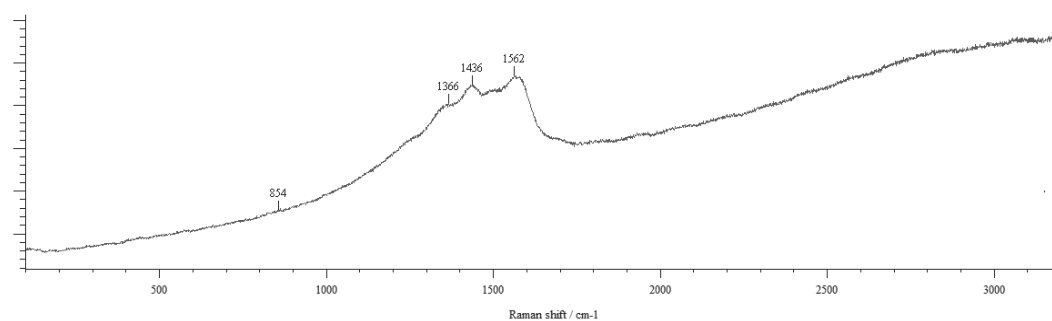


Fig. 8. Raman spectra of the PEDOT:PSS prepared from solution T

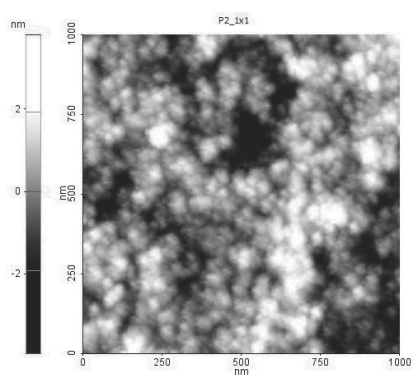


Fig. 9. AFM image of the surface topography of P2 sample

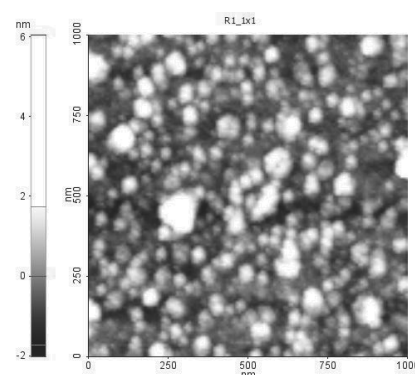


Fig. 11. AFM image of the surface topography of R2 sample

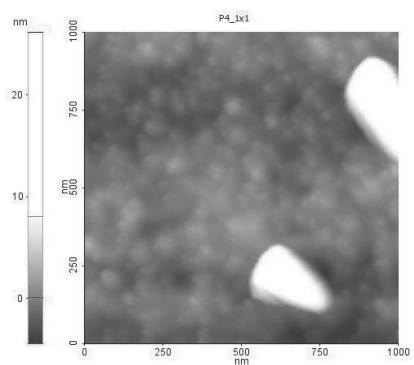


Fig. 10. AFM image of the surface topography of P4 sample

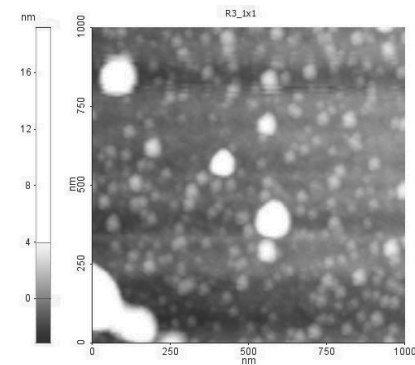


Fig. 12. AFM image of the surface topography of R4 sample

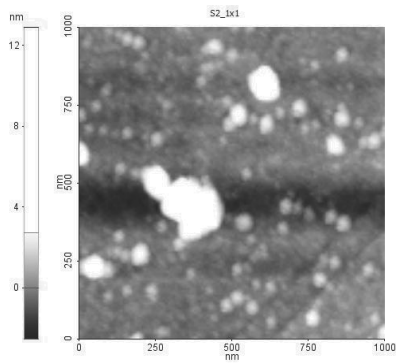


Fig. 13. AFM image of the surface topography of S2 sample

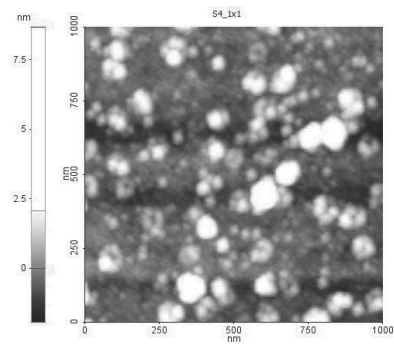


Fig. 14. AFM image of the surface topography of S4 sample

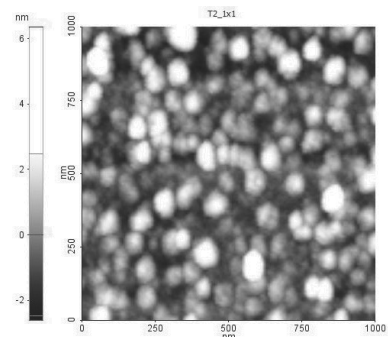


Fig. 15. AFM image of the surface topography of T2 sample

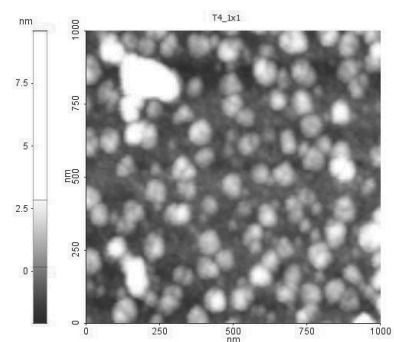


Fig. 16. AFM image of the surface topography of T4 sample

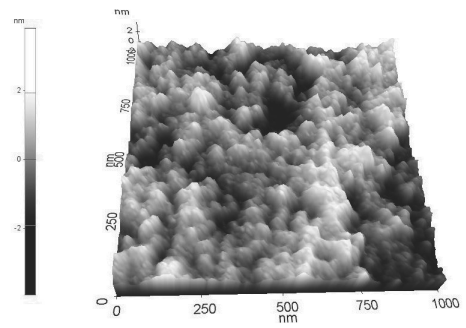


Fig. 17. AFM 3D image of the surface topography of P2 sample

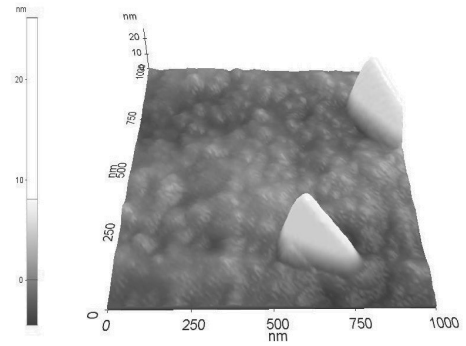


Fig. 18. AFM 3D image of the surface topography of P4 sample

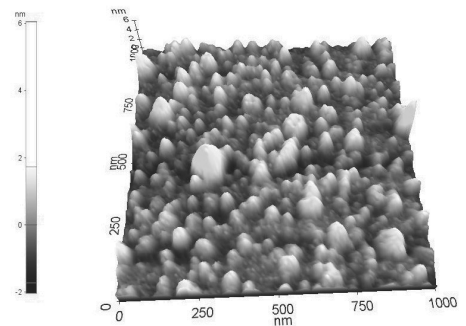


Fig. 19. AFM 3D image of the surface topography of R2 sample

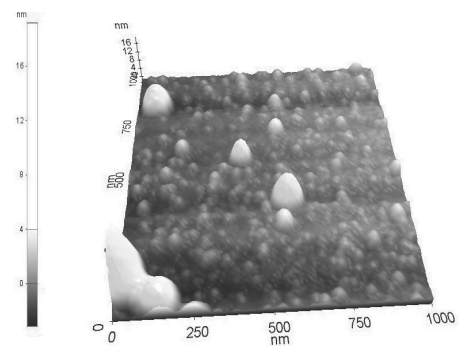


Fig. 20. AFM 3D image of the surface topography of R4 sample

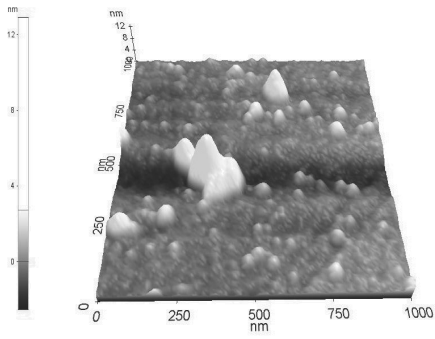


Fig. 21. AFM 3D image of the surface topography of S2 sample

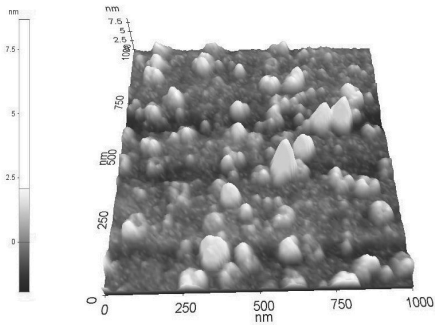


Fig. 22. AFM 3D image of the surface topography of S4 sample

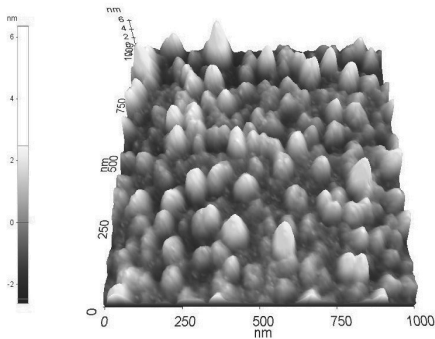


Fig. 23. AFM 3D image of the surface topography of T2 sample

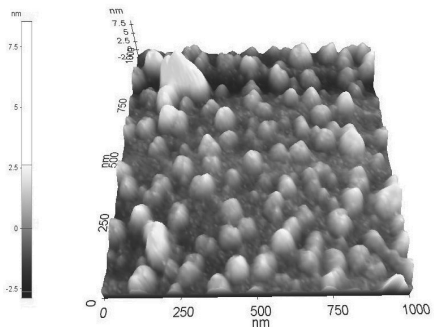


Fig. 24. AFM 3D image of the surface topography of T4 sample

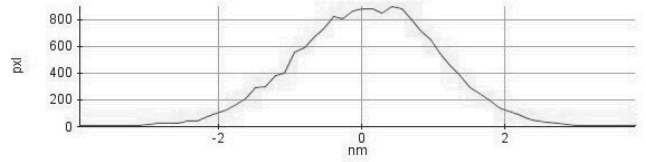


Fig. 25. The histogram of frequency of the occur height for a P2 sample

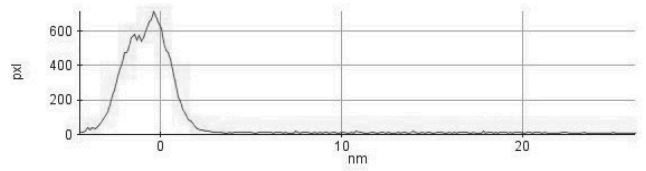


Fig. 26. The histogram of frequency of the occur height for a P4 sample

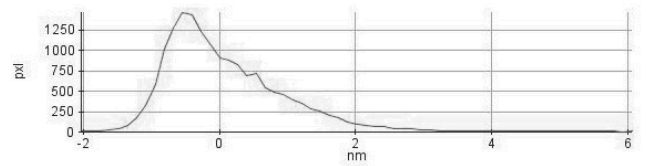


Fig. 27. The histogram of frequency of the occur height for a R2 sample

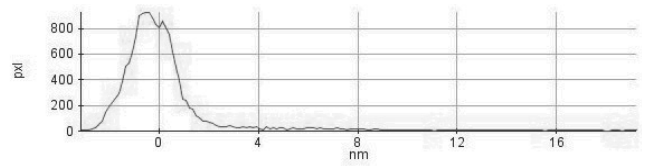


Fig. 28. The histogram of frequency of the occur height for a R4 sample

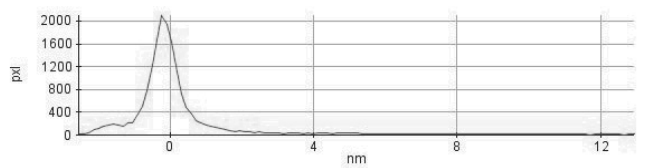


Fig. 29. The histogram of frequency of the occur height for a S2 sample

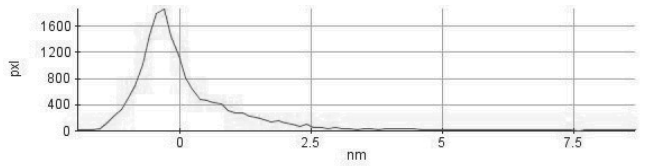


Fig. 30. The histogram of frequency of the occur height for a S4 sample

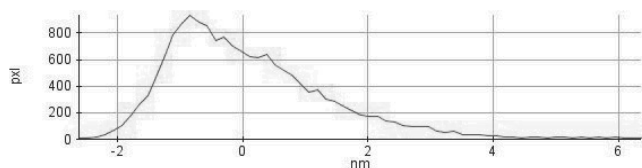


Fig. 31. The histogram of frequency of the occur height for a T2 sample

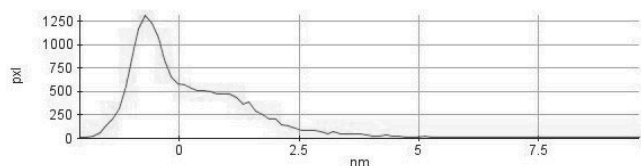


Fig. 32. The histogram of frequency of the occur height for a T4 sample

Fig. 33 shows measured and modelled ellipsometric spectra of PEDOT:PSS. Refractive index measured at a wavelength of 632.8 nm was 1.655 respectively.

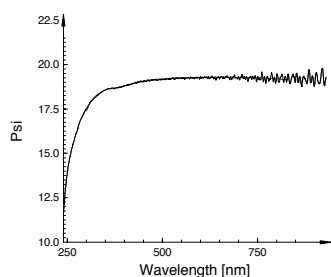


Fig. 33. Measured and modelled ellipsometric spectra ($\Phi = 70^\circ$) of PEDOT:PSS

The UV/VIS spectrometer was used to investigate absorbance of the obtain thin films. The absorbance was below 0.04 in the wavelength range 350-950 nm (Fig. 34).

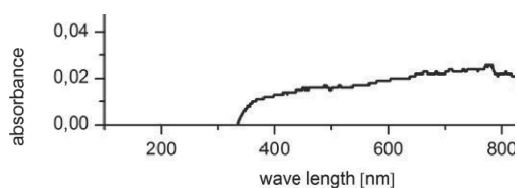


Fig. 34. Spectral absorbance curve for P2 PEDOT:PSS thin film

4. Conclusions

Research of surface morphology by using AFM has confirmed possibility to obtain uniform thin films. Research with using a spectrometer UV/VIS and spectroscopic ellipsometer has confirmed favorable optical properties of PEDOT:PSS. The

results may lead to the conclusion that PEDOT:PSS can be used in photovoltaic and optoelectronic devices.

Acknowledgements

Magdalena Szindler is a holder of scholarship from project POKL.08.02.01-24-005/10 entitled: "Scholarships Support Innovative Technology Forum (SWIFT)".

References

- [1] J.E. McMurry, Organic chemistry, Eighth Edition, International Edition, 2011.
- [2] L. Dai, Intelligent macromolecules for smart devices, Springer, London, 2004.
- [3] W. Torbicz, D. Pijanowska, Electroconductive polymers in electronics and analytical biochemical, Electronics 6 (2009) 36-43.
- [4] I. Gruin, Polymeric materials, Publishing House PWN, Warsaw, 2003.
- [5] J.A. Mikroyannidisa, M.M. Stylianakisa, M.S. Royc, P. Sureshb, G.D. Sharmab, Synthesis, photophysics of two new perylene bisimides and their photovoltaic performances in quasi solid state dye sensitized solar cells, Journal of Power Sources 194/2 (2009) 1171-1179.
- [6] L.A. Dobrzański, M. Musztyfaga, A. Drygała, W. Kwaśny, P. Panek, Structure and electrical properties of screen printed contacts on silicon solar cells, Journal of Achievements in Materials and Manufacturing Engineering 45/2 (2011) 141-147.
- [7] A. Proń, Synthetics metals, Knowledge and Life 2, 2001.
- [8] S.E. Burkhard, Theoretical and Electrochemical Analysis of Poly(3,4-alkylenedioxythiophenes), Electron-Donating Effects and Onset of p-Doped Conductivity, Journal of Physical Chemistry C 114 (2010) 16776-16784.
- [9] H. Shirakawa, E.J. Louis, A.G. MacDiarmid, C.K. Hiang, A.J. Heeger, Synthesis of Electrically Conducting Organic Polymers, Journal of the Chemical Society, Chemical Communications (1977) 578-580.
- [10] H. Shirakawa, Synthesis and characterization of highly conducting polyacetylene, Synthetic Metals 69 (1995) 3-8.
- [11] J. Weszka, M.M. Szindler, M. Chwastek-Ogierman, M. Bruma, P. Jarka, B. Tomiczek, Surface morphology of thin films polyoxadiazoles, Journal of Achievements in Materials and Manufacturing Engineering 49/2 (2011) 224-232.
- [12] J. Weszka, M.M. Szindler, M. Bruma, Surface morphology and optical properties of polymer thin films, Electronics 6 (2012) 120-122.
- [13] J. Weszka, M. Szindler, A. Śliwa, B. Hajduk, J. Jurusik, Reconstruction of thin films polyazomethine based on microscopic images, Archives of Materials Science and Engineering 48/1 (2011) 40-48.
- [14] K. Norrman, A. Ghanbari-Siahkali, N.B. Larsen, Studies of spin-coated polymer films, Annual Reports C 101 (2005) 174-201.
- [15] S. Xiao, S. Abreu Fernandes, C. Esen, A. Ostendorf, Picosecond Laser Direct Patterning of Poly(3,4-ethylene dioxythiophene)-Poly(styrene sulfonate) (PEDOT:PSS)

- Thin Films, Journal of Laser Micro/Nanoengineering 6/3 (2011) 249-254.
- [16] L.A. Dobrzański, M. Szindler, Sol-gel and ALD antireflection coatings for silicon solar cells, Electronics 8 (2012) 125-127.
- [17] F. Zhi-Hui, Polymer solar cells based on a PEDOT:PSS layer spin-coated under the action of an electric field, Chinese Physics B 19/3 (2010) 038601.
- [18] J. Gasiorowski, Surface morphology, optical properties and conductivity changes of poly(3,4-ethylenedioxythiophene): poly(styrenesulfonate) by using additives, Thin Solid Films 536 (2013) 211-215.
- [19] J. Weszka, Influence of technological conditions on electronic transitions in chemical vapour deposited poly(azomethine) thin films, Thin Solid Films 516 (2008) 3098-3104.